INTERNATIONAL JOURNAL OF HYDROGEN ENERGY 48 (2023) 32553–32571

Available online at www.sciencedirect.com

ScienceDirect

journal homepage: www.elsevier.com/locate/he

# Feasibility analysis of a direct injection $H_2$ internal combustion engine: Numerical assessment and proof-of-concept

*Alessio Anticaglia* [a], *Francesco Balduzzi* [a,*], *Giovanni Ferrara* [a], *Michele De Luca* [b], *Davide Carpentiero* [b], *Alessandro Fabbri* [b], *Lorenzo Fazzini* [b]

[a] *Department of Industrial Engineering, Università degli Studi di Firenze, Via di Santa Marta 3, Firenze, 50139, Italy*
[b] *HPE-COXA, Via Raimondo Dalla Costa 620, Modena, 41122, Italy*

## HIGHLIGHTS

- Dedicated thermo-fluid dynamic design of a $H_2$ICE.
- Influence of compression ratio in turbocharged $H_2$ICE was examined.
- The performance can be increased with delayed injection timings.
- Strategies for optimal Low End Torque performance in lean burn $H_2$ICE.
- Effect of low-tumble intake ports and VVT was studied.

## GRAPHICAL ABSTRACT

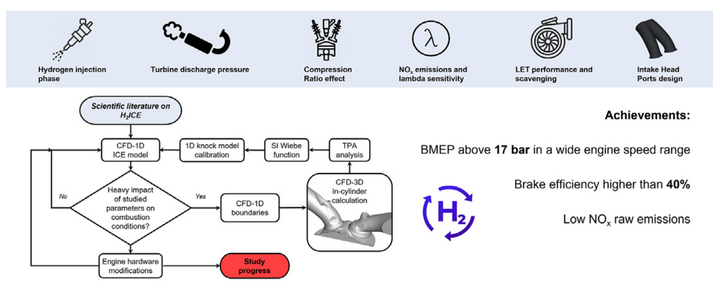


## ARTICLE INFO

*Article history:*
Received 2 January 2023
Received in revised form
21 April 2023
Accepted 28 April 2023
Available online 20 May 2023

*Keywords:*
Internal combustion engines
Hydrogen
H2-ICE
Alternative fuels

## ABSTRACT

The present study is a proof-of-concept investigation of a lean hydrogen internal combustion engine aiming to understand and address its critical thermo-fluid dynamics aspects, by means of a multi-fidelity computational fluid dynamics approach. Starting from an existing gasoline engine, the influence of the most relevant parameters and components on performance and efficiency is investigated using both one- and three-dimensional simulation tools, with the goal of defining a comprehensive strategy for adapting the engine design to the new requirements imposed by the hydrogen fuel. In particular, the following parameters affecting the retrofit effectiveness are analyzed and modified by the authors: turbocharging system, injection strategy, compression ratio, valves timing and intake ports design. Promising performance are achieved with the final configuration, revealing that substantial improvements can be obtained through a

* *Corresponding author.*
E-mail addresses: alessio.anticaglia@unifi.it (A. Anticaglia), francesco.balduzzi@unifi.it (F. Balduzzi), giovanni.ferrara@unifi.it (G. Ferrara), mdeluca@hpe.eu (M. De Luca), dcarpentiero@hpe.eu (D. Carpentiero), afabbri@hpe.eu (A. Fabbri), lfazzini@hpe.eu (L. Fazzini).
https://doi.org/10.1016/j.ijhydene.2023.04.339

dedicated design: the BMEP is consistently above 17 bar with a peak brake efficiency higher than 40%.



**Acronyms and abbreviations**

| | |
|---|---|
| *CFD* | Computational Fluid Dynamics |
| *DOE* | Design Of Experiments |
| *KPI* | Key Performance Indicators |
| *CR* | Compression Ratio |
| *BDC* | Bottom Dead Center |
| *bBDC* | Before Bottom Dead Center |
| *aBDC* | After Bottom Dead Center |
| *TDC* | Top Dead Center |
| *TDCe* | Top Dead Center exchange |
| *TDCf* | Top Dead Center firing |
| *bTDC* | Before Top Dead Center |
| *aTDC* | After Top Dead Center |
| *BMEP* | Brake Mean Effective Pressure |
| *IMEP* | Indicated Mean Effective Pressure |
| *PMEP* | Pumping Mean Effective Pressure |
| *FMEP* | Friction Mean Effective Pressure |
| *MPS* | Mean Piston Speed |
| *BSFC* | Brake Specific Fuel Consumption |
| *CD* | Discharge Coefficient |
| CoC | Center of Combustion |
| *MBF* | Mass Fraction Burned |
| *MBF*50 | Mass Fraction Burned of 50% |
| *MBT* | Maximum Brake Torque |
| *DI* | Direct Injection |
| *GDI* | Gasoline Direct Injection |
| *H2DI* | Hydrogen Direct Injection |
| *PFI* | Port Fuel Injection |
| *SOI* | Start of Injection |
| *EOI* | End of Injection |
| *SI* | Spark Ignition |
| *CI* | Compression Ignition |
| GHG | Greenhouse Gases |
| *ICE* | Internal Combustion Engine |
| *ICEV* | Internal Combustion Engine Vehicle |
| *HEV* | Hybrid Electric Vehicle |
| *PHEV* | Plug-In Hybrid Electric Vehicle |
| *BEV* | Battery Electric Vehicle |
| *FCEV* | Fuel Cell Electric Vehicle |
| *FWD* | Front Wheel Drive |
| *DCT* | Dual Clutch Transmission |
| *LCA* | Life Cycle Assessment |
| *PID* | Proportional-Integral-Derivative |
| *LET* | Low End Torque |
| *LSPI* | Low Speed Pre-Ignition |
| *LFS* | Laminar Flame Speed |
| *RON* | Research Octane Number |
| *MON* | Motor Octane Number |
| *TWC* | Three Way Catalyst |
| *SCR* | Selective Catalytic Reduction |
| *PR* | Pressure Ratio |
| *VVT* | Variable Valve Timing |
| *VGT* | Variable Geometry Turbocharger |
| *WOT* | Wide Open Throttle |
| *MAP* | Manifold Absolute Pressure |
| *IAT* | Intake Air Temperature |
| *TET* | Turbine Entry Temperature |
| *WG* | Wastegate |
| *KI* | Knock Index |
| *KL* | Knock Limit |
| *IVO* | Intake Valve Opening |
| *EVO* | Exhaust Valve Opening |
| *IVC* | Intake Valve Closing |
| *EVC* | Exhaust Valve Closing |
| *ITA* | Intake Timing Advance |
| *ETD* | Exhaust Timing Delay |
| *SA* | Spark Advance |
| *WLTP* | Worldwide Harmonized Light Vehicle Test Procedure |
| RDE | Real Driving Emissions |

## Introduction

Over the last years, the society has been undergoing substantial changes related to a more sustainable energy management. The automotive field, as one of the key players in the energetic transition, is asked to develop new technologies and concepts to minimize carbon impact on the planet. At the present time (Euro 6 regulations), regulators require emission compliance only by means of a tailpipe emission test measured with specific testing procedures, such as the Worldwide.

Harmonized Light Vehicle Test Procedure (WLTP) and Real Driving Emission (RDE) approval protocols, resulting in zero emissions certification for non-fuelled vehicles. It seems reasonable to assume that, in a very soon future, besides increasingly stringent homologation vehicular standards, the real carbon footprint of the vehicle will be accounted considering all the processes related with the vehicle life, which means using the Life Cycle Assessment (LCA) method. While some studies support the rapid transition to all-electric light-duty vehicle fleets, many researches declare that, considering the real carbon footprint of a vehicle through the LCA method [1–3], the most relevant alternatives to Battery Electric Vehicles (BEVs) are Full Hybrid Electric Vehicles (FHEVs) and Plug-in Hybrid Electric Vehicles (PHEVs) especially considering the easier, and less energy-intensive, processes associated with infrastructure conversion as well as vehicle production and dismantling.

Within this context, latest researches in e-fuels further corroborate investments in these type of vehicle architectures, allowing to pursue the carbon neutrality without the need of completely upsetting the power distribution network. Therefore, Internal Combustion Engines (ICEs) still have a role to play in reducing Greenhouse Gas (GHG) emissions in the coming years.

Considering also the simplicity (for the final user) and the celerity of the refueling method, which can smoothly compensate the vehicle short range, the primary goal of this work is to investigate whether or not a Hydrogen fuelled Internal Combustion Engine Vehicle (ICEV) is a good alternative to other solutions in a short-time basis and, more importantly, which type of issues are associated with these types of vehicles and engines. Many scientific articles investigate specific problems related to the hydrogen retrofitting of an existing internal combustion engine. Most of these numerical investigations are focused on specific aspects namely the mesh methodology to correctly simulate in-cylinder effects [4,5], the right injection technology to achieve optimal performance [6], combustion models [7,8], the occurrences of abnormal combustion in hydrogen mixtures [9,10], the determination of burning velocities of hydrogen mixtures [11–13,15] along with others [14,16,17]. On the other hand, other investigations deal with technological retrofitting challenges such as injection system components design [6,18], cranktrain components design considering mechanical behaviour of materials in presence of hydrogen (such as embrittlement, analyzed in Ref. [19]), ignition technologies [20]. What is not completely clarified by the general bibliography is how to summarize all these points at a system level from the design phase and how to exploit the full potential of these unique fuel properties with tailored choices. Starting from the comprehension of well known key effects of Hydrogen Internal Combustion Engines (*H*2-ICEs) described in scientific literature, this work presents a quite detailed, albeit strictly numerical, engine design methodology defined analyzing the effect of the most relevant parameters to obtain power density targets comparable with current turbocharged Spark-Ignition (SI) engines for B and C segment passenger cars. For each Key Performance Indicator (KPI), summarized in Fig. 1, a set of detailed analysis was performed to comprehend and show in detail what are the consequences for the entire engine and then how to take advantage of them to reach target performance.

Finally, strategies to obtain high brake efficiency and low nitrogen oxides (*NOx*) raw emissions are studied to guarantee best compromise behaviour for road propulsion applications.

All these aspects are not covered in such a way in the existing literature, hence it is the focus of the present work.

## Case study

The engine model used as a starting point for the present work was derived from a high performance turbocharged engine for supercar applications. Being a V6 engine layout, each bank is fluid dynamically independent from the other; this means that 1D simulations can be performed on a single bank for computational reasons. Interaction between different cylinders of the same bank, peculiar of this type of engine layout and firing order, in fact are correctly simulated within the numerical model, while the interaction between the two banks is only mechanical, hence negligible for this work purposes. The presented engine model has been selected essentially as a robust, numerically correlated, starting point. For confidentiality reasons all relevant features, data and results are presented in a non dimensional form. The full load performance curve of the baseline engine is presented in Fig. 2 in terms of Brake Mean Effective Pressure (BMEP) versus Mean Piston Speed (MPS). The specifications of the cylinder unit are summarized in Table 1.

During the numerical hydrogen conversion process, fundamental aspects of the engine were redefined in order to fit the specific application needs. Among all, the most relevant ones are: mean piston speed range, exhaust line properties, compression ratio (CR), piston crown shape, intake head ports design, injector type. The turbocharger selection deserves a separate discussion; starting from the target maximum power

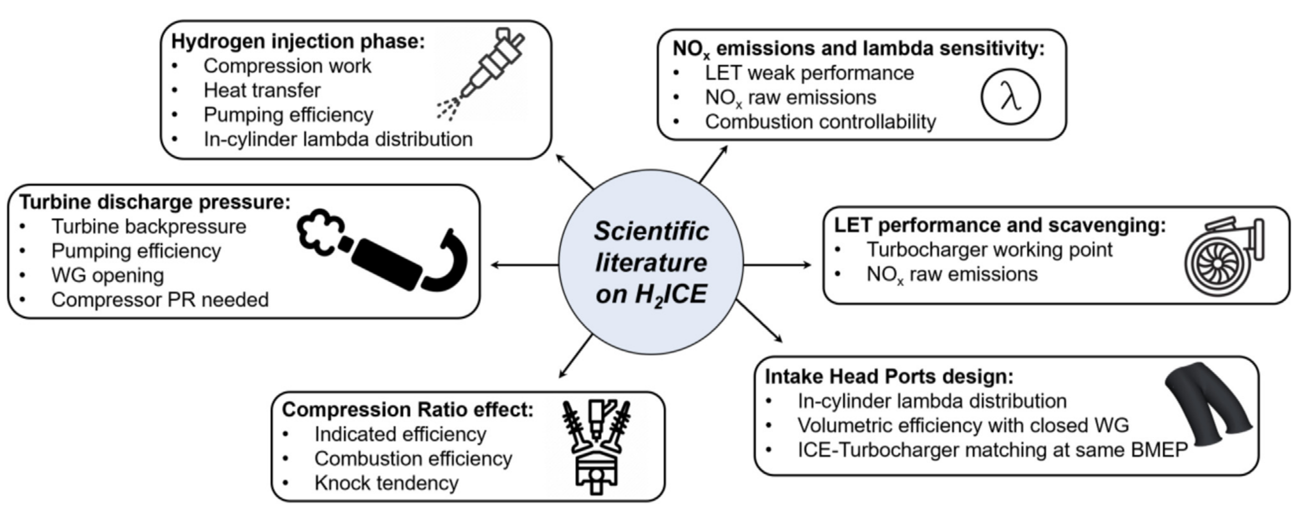


**Fig. 1 – Study analysis.**

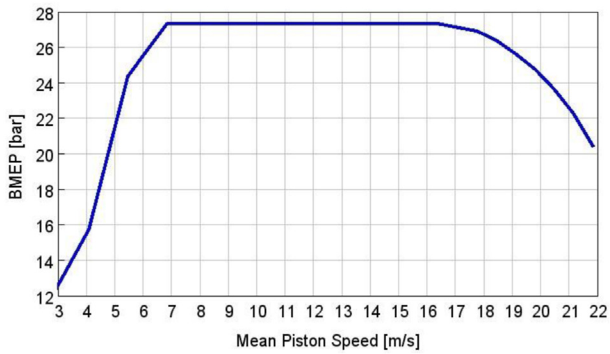


**Fig. 2 – Baseline engine performances: BMEP as a function of the MPS.**

**Table 1 – Baseline engine cylinder unit properties.**

| Parameter | Parameter |
|---|---|
| Bore/Stroke | 1.07 |
| Crank radius Connecting rod length | 0.26 |
| Compression Ratio | 9.3:1 |
| Number of intake valves per cylinder | 2 |
| Number of exhaust valves per cylinder | 2 |
| Charge motion approach | High Tumble |
| Injection system | Direct |
| Maximum IMEP720 | 29.6 bar |
| Maximum BMEP | 27.3 bar |
| Maximum MPS | 21.9 m/s |

output and a minimum lambda value of 2.0 at full load, the ideal turbocharger size and technology, for the scope of this research, was investigated. Making use of Turbomachinery Similitude Theory [21–25], internal know-how and expertise gained from previous experiences [26,27], a single stage wastegate turbocharger resulted eligible for this application.

Thus, for the scope of this study, no advanced turbocharging systems were deemed necessary. It appears clear to the authors that, for extreme applications, a two stage intercooled compression could be necessary to obtain relevant values of BMEP; alternatively, a single stage high-flow compressor can be used in conjunction with electrified solutions (e-turbo) to drive the compressor at low flow rates and, possibly, use the electric motor instead of the wastegate to limit the turbomachine speed.

What authors evidently noticed is that in part load and, in general, using leaner mixtures, exhaust gases temperature falls down. As a consequence, different lambda constraint at full load for the engine concept or hybrid powertrain layouts, for which the ICE technical definition could be better optimised focusing on a narrower operating range, can lead the way to variable geometry turbine technologies or electrified turbocharging solutions. Certainly these technologies will be one of the future area of interest.

As a result of the above, a direct comparison between the proposed dimensionless curve and the one of the Hydrogen version is meaningless because the engine mission profile, the hardware selected and the goals perceived during the engine development are deeply unrelated.

## Design practice

Moving from an extended literature survey, the present study proceeds with the comprehension of effects and implications on the engine operation of specific aspects, in particular:

(1) Hydrogen injection phase
(2) Turbine discharge pressure
(3) Compression Ratio effect
(4) *NOx* emissions and lambda sensitivity
(5) Low End Torque (LET) performance and scavenging
(6) Intake Head Ports design

### *Hydrogen injection phase*

The injection phase is key in a *H*2-ICE, resulting in one of the most relevant difference with gasoline engines. Due to the low density of this fuel, Port Fuel Injection (PFI) systems produce significant, yet undesired, effects on the volumetric efficiency causing reduced power outputs [28–33]. In addition to that, experimental analyses reported in literature [2,16,32,34–37] have shown the occurrence of backfiring in the intake pipe when increasing the engine load or reducing mixture lambda from lean mixtures toward stoichiometric conditions. It is worth pointing out that these occurrences are a clear consequence of three physical properties of hydrogen: wide ignition limits, low activation energy for the combustion reactions, high Laminar Flame Speed (LFS). Direct Injection systems and closed-valves injection timings appear the preferable solution toward competitive performances and operation safety [29,30]. Hydrogen Direct Injection (*H*2-DI) technology nonetheless offers additional degree of freedom compared to other concepts, but adds complexity both to the engine control and the numerical investigation due to involved in-cylinder phenomena [30]. The main challenge is a proper mixture formation, cycle variation, NOx formation and abnormal combustions (pre ignition) [38,39]. Practically, *H*2-DI engines require innovative and tailored injection components and introduce a tough technical problem: guarantee high static flow rates needed to obtain the desired lambda, a good homogenization and the latest injection phase possible [30,40,41]. Injection timing and duration appear hence crucial parameters for these applications. This first part of the study, presented in the Chapter 5.1, suggests how much the injection phase is associated with considerable losses caused by the energy needed for the compression stroke. Evaluations were made at fixed intake conditions and in-cylinder mixture properties, i.e. the same levels of Manifold Absolute Pressure (MAP), Intake Air Temperature (IAT) and trapped lambda.

### *Turbine discharge pressure*

For hydrogen-air mixtures, the unique polluting substance released during the combustion are nitrogen oxides, which are released under high pressure and high temperature conditions. Nevertheless, carbon compounds, hydrocarbons mid-products and particle emissions can be present at the exhaust due to the burning of lubricant oil (as experimentally studied in Ref. [16]). However, to numerically address this problem, a deep level of detail is needed. Specific oil formulations for hydrogen engines need to be known and more appropriate combustion models must be employed. In addition to that, further investigations have to be conducted regarding crack-case ventilation systems, H2 slip into crankcase occurrences [31,40], piston mechanical design and thermal behaviour, compression rings and oil control rings design choices and materials (considering embrittlement phenomena, as per Ref. [24,38,40]) along with clearance between piston and cylinder wall. Thus, for the purpose of this study we ignored the effect of lubricant oil contaminations. Under these assumptions, products of the air-hydrogen mixtures combustion are hence carbon free, with the consequence that aftertreatment devices needs are way different from what generally seen in modern gasoline engines, such as pre-cat, Three-way catalyst (TWC), Gasoline Particulate Filter (GPF) and eventually De-*NOx* Selective Catalytic Reduction (SCR) Catalyst [30,42]. Therefore, for such an application, typical levels of turbine discharge pressure (turbine backpressure, not engine backpressure) of an EU6 turbocharged Gasoline Direct Injection (GDI) engine are unrealistic and excessive. The turbine backpressure, in actual fact, is a direct consequence of the exhaust permeability: pipes design and the aftertreatment devices (as concentrated pressure losses); the engine backpressure, conversely, includes the effect of the turbine and, clearly, for a heavily turbocharged and lean operated engine, is significant. Regarding *NOx* emissions, it is worth reminding that they must be limited, first and foremost, during the combustion phase itself; it means making use of all the conventional techniques applied in Diesel or gasoline engines. In particular, spark timing, effective CR, trapped lambda, Exhaust Gas Recirculation (EGR) rate, intake charge conditions in addition to the aforementioned Start Of Injection (SOI) have a great effect on the *NOx* raw emission levels. Conventional *NOx* aftertreatment devices, such as SCR systems can also be used, as shown in some investigations [30,40,43]. These devices were not considered in this work for two main reasons. The first one is that the selection of these components and hence the consequences for the engine are highly related with the engine-vehicle matching, the homologation test procedure and limits (WLTC and RDE testing procedures and Euro 7 homologation limits). All these aspects were not clear at the date of this work and, in general, are far from the aim (a "conceptual development") pursued in this study. The second aspect is that these systems need specific adjustments to work with the new exhaust composition and the thermal window found with hydrogen applications. Detailed and reliable information about the sizing and the effect of these components were unavailable when these analyses were conducted.

Considering the above, within the present analysis, four different exhaust lines were tested to address the effect of the turbine backpressure on performance and engine design:

(1) an exhaust line having the same turbine backpressure level as the one used with the baseline gasoline engine (worst case scenario).
(2) the same exhaust line used in the baseline engine; pressure drops along the entire exhaust line however are the result of the different composition and thermodynamic conditions of the exhaust gases. It means that the effective turbine backpressure, also with same trapped air mass per cycle, could be different with respect to the reference engine.
(3) a very permeable line, meaning that at the maximum power operating point the pressure drop along the exhaust is only 200 mbar.
(4) a straight pipe, meaning that no additional concentrated pressure loss sources are accounted. This line represents a typical racing exhaust and, in general, was introduced only to evaluate the response of the system with these type of exhaust conditions. It is clear that, in view of street legal applications, these values of backpressures are not reasonable.

It seems realistic to the authors that a feasible exhaust line for such an engine could be a mix between the second and the first lines presented. Even in this evaluation, as suggested in literature, the engine was operated with mixture dilution of lambda 2.0 in Wide Open Throttle (WOT). With these values of oxygen excess, *NOx* emissions are extremely reduced also in presence of high pressure peaks.

### *Compression ratio effect*

In modern conventional SI engines, low speeds and high loads is the most critical operating condition with respect to knock phenomena and, in a broad sense, abnormal combustion occurrences (pre-ignitions, Low Speed Pre-Ignition (LSPI), mega-knock, etc) are limiting both the performance and the engine efficiency [24,25]. On the contrary, LFS of hydrogen mixtures, even at lambda 2.0, is far higher than that of gasoline-air mixtures resulting in a weaker dependence of knock tendency with respect to the charge turbulence level and so to the engine speed. A typical turbocharged GDI engine compression ratio could be thus moderate for a lean burn *H2*-ICE, especially in view of an efficiency-oriented machine that is the aim of the whole study [13,37,42,44]. Low compression ratio, anyway, could be pursued in extreme applications where, due to as stoichiometric as possible mixtures or extremely high supercharging levels, pressure peaks are intense and abnormal combustion conditions quickly become severe and persistent, commanding to reduce the compression ratio albeit deteriorating the efficiency. The non-appearance of combustion anomalies with lean mixtures, reported in scientific literature and confirmed by 3D calculations, opens up the possibility to higher the compression ratio with expected advantages of efficiency in WOT and, more importantly, at part loads which are the most frequently operated points in a vehicle oriented internal combustion engine. A new value of 12.0:1 CR was selected as a best compromise between fluid dynamics needs (evaluated with a synergic use of 1D and 3D codes) and the mechanical constraints defined by combustion chamber design, piston weight, valve recesses; this new compression ratio was admittedly obtained redesigning only the piston crown in view of easy conversion of the starting engine for testing campaigns. It must be noted that a different piston should be adopted anyway to safely cope with the higher pressure peaks reached in this application.

### NOx *emissions and lambda sensitivity*

Hydrogen mixtures, differently from gasoline ones, are characterized by a wide flammability range; this aspect drove many researches reported in scientific literature to investigate the optimal lambda value to fuel the engine for the performance [45]. The wide mixture lambda operability, which means the possibility to control the engine load by quality, is also frequently presented as one of the real main advantages of these type of engines in comparison with conventional ones [35]. The expected, and experimentally proven, reduction in efficiency decrement over the entire engine map, in fact lead to huge advantages for the customer and the environment.

In order to evaluate how to correctly assess inferior lambda limits to operate the engine in the mentioned Low End Torque (LET) zone, a set of different operating points was selected and simulated with the one-dimensional numerical model. All points were evaluated at 2000 rpm with different levels of valve overlap and different values of trapped lambda at the Intake Valve Closing (IVC). These points were used to extract sets of boundary conditions to be used for the in-cylinder 3D combustion calculation. For each operating point a spark sweep until knock limit spark advance was simulated to compute how much Indicated Mean Effective Pressure (IMEP), efficiency and *NOx* production are affected by the combustion phase [45]. Within the simulated cases, the Intake Valve Closing (IVC) variation produces different internal EGR rates, effective compression ratio and trapped lambda for each case resulting in a quite heterogeneous analysis of main parameters affecting nitrogen oxides production. The use of a detailed combustion chemistry model allowed a quantitative evaluation of *NOx* emission trends and directed the next steps of the research.

### *LET performance and scavenging*

To address LET performance problems an investigation of the effect of the scavenging process in this specific operating zone was conducted. The scavenging, which means virtually increasing the volumetric flow rate elaborated from the engine inducing a consistent valve overlap, is a well known way to increase performance in turbocharged engines. In PFI gasoline engines this solution originates high specific fuel consumption as a consequence of the decrement in trapping efficiency; with GDI engines, where these problems are not present, a wide overlap is incompatible with the mixture requirements for the correct operation of three way catalyst. The new aftertreatments constraints (presented in the Chapter 3.2), however, do not require strict stoichiometric conditions making possible the use of the presented strategy. In addition to that, it should be noted that the reduction of lambda (with respect to the selected value of 2.0) is an easy way to increase the power output limitedly to these critical zones of operation. Theoretically the inferior limit is dictated by the combustion controllability and the raw emission levels. Aside from these aspects, there is a noticeable advantage in using lean mixture related with combustion, adiabatic and pumping efficiencies (following Ref. [23] definitions). This is the reason why, besides low nitrogen oxides emissions, it is preferable to operate with ultra lean mixtures along with load regulation by quality whenever possible [45]. Nonetheless, in this operating zone, a slight reduction of the trapped lambda can bring to consistent performance increments; as a consequence, the investigation was performed at different levels of trapped lambda (from 1.7 to 2.0). From an operational perspective, a broader valve overlap can be effortlessly obtained exploiting the Variable Valve Timing (VVT) system on both intake and exhaust camshafts. Advancing the intake profile or delaying the exhaust one in fact produce, among other things, a gain in valve overlap. By contrast, inducing overlap only by means of the VVT actuation, intake and exhaust phases and the effective compression ratio (valve closure event dependant) are affected by the same token, with repercussions to be scrupulously valued. Nevertheless, considering the good fluid dynamics behaviour of baseline intake and exhaust valves profiles in practically the whole piston mean speed range, as well as the good mechanical integration and organic efficiency of the complete valvetrain, this study will investigate the effect of the scavenging obtained only adjusting the VVT device. After an initial phase of sensitivity analysis towards scavenging and model setup, the operating points of major interest were selected implementing a Design Of Experiments procedure on VVTs. Both intake and exhaust cam timings were concomitantly used to induce scavenging on the engine, while angular adjustment limits were defined according to the maximum valve lift permitted at the Top Dead Center exchange (TDCe).

### *Intake head ports design*

In modern turbocharged GDI engines, intake ports are typically designed to maximize tumble. The tumble charge motion is certainly one of the main parameters to speed up the combustion rate with all the advantages related to indicated efficiency, combustion completeness and knock tendency. This type of charge motion is obtained with specific design of the intake ports, injector location and piston bowl geometry; high tumble ports however tends to reduce the permeability of the intake line limiting the volumetric efficiency. This problem nevertheless is typically not so relevant because of the margin offered by compressor to adjust the boost pressure. In conclusion, in conventional GDI engines, advantages offered by a high tumble oriented port design oversee the disadvantages.

Hydrogen engines, on the contrary, exhibit three major differences. They have a narrow margin in compressor operation due to the low turbine enthalpy, they require high volumetric efficiency to guarantee good performances at lean conditions and they are characterized by high laminar flame speeds also in presence of considerable oxygen excess [11,15,42,46]. As a result, the combustion duration is less dependent on the turbulence level. On these bases, it appears reasonable to evaluate the effect of a permeable intake duct.

Theoretically this operation could led to:

- increment the performance in the LET zone
- increment of efficiency in the remainder zone of the operating map

In the LET zone in fact, considering same operating parameters (SOI, VVT actuation, trapped lambda, combustion center) and a close position of the wastegate actuator, the increment of performance is associated with a decrease in intake pressure losses. In addition to that, the new head design could bring to better homogenization of the mixture, providing an opportunity for delayed SOI timings and a better flame propagation. These latter aspects were, actually, investigated and confirmed exploiting the 3D combustion calculation. Concerning the widespread increment of efficiency, it appears reasonable because of less pumping losses and a more centred use of the turbocharger. As previously reported, from a certain engine speed value up to the rev limiter the boost pressure obtained is sufficient to guarantee required torque values at lambda 2.0, even more so with the new head design. Actually, the supercharging level offered is more than enough, at the point that it is necessary to open the wastegate valve to limit the torque at the required amount, as usual with turbocharged engines.

## Methods and validation

### CFD-1D

The entire investigation was conducted using mainly the one-dimensional unsteady gas dynamics commercial software GT-Power (v2016), from the Gamma Technologies package. The solution is obtained using the direct method (explicit solver).

Using this method the relationship between timestep and discretization length is determined making use of the Courant number.

Consequently, the timestep is determined so that:

$$\frac{\Delta t}{\Delta x}(|u|+c) <= 0.8 * m \tag{1}$$

With:

- $\Delta t$: timestep ($s$).
- $\Delta x$: minimum discretization length ($m$).
- u: fluid velocity ($m/s$).
- c: sound velocity ($m/s$).
- m: corrective constant for the timestep defined by the user (equal or minor to 1).

As frequently needed with 1D methods, the entire model development was supported by 3D calculations, using the commercial code Star-CCM+(v15.06), to evaluate local effects in specific components. In fact, considering the complex phenomena of the flow through the head ports, across valve guides and its interaction with valves and cylinder liners at different valve heights, the calculation of discharge coefficients for the intake and exhaust head ports was performed with 3D CFD models. Similarly, the estimation of pressure losses across the intercooler, throttle body and all exhaust components (pre-cat, TWC, GPF, silencer) for the baseline engine model creation was investigated using this method; results of these steady-state calculations then drove the calibration of friction multipliers and discharge coefficients within the GT-Power model. The fuel model used in the GT-Power code reflects the exact properties of the fuel used for test bench analyses. The 1D reference model was hence validated on test bench data of the original GDI engine to assess the level of accuracy needed to use the code with confidence. For each cylinder of the test engine, a Kistler 6054C PiezoStar cylinder pressure sensor was installed. This sensor presents a high natural frequency, therefore the effect of engine vibrations on the measurement quality is minimal. Fig. 3 reports the correlation between baseline 1D model trends and experimental results from the fully instrumented engine, in terms of Clapeyron diagram (with log-log scale to emphasize the pumping loop).

Minutely, for the pumping cycle and the power cycle the maximum deviation of numerical with respect to the experimental is below 0.8% and 1% respectively. The consistency and the prediction capability of the model used as the starting point of the entire work proposed can hence be confirmed.

For the purposes of this study, within the one-dimensional code, the combustion process is simulated using a non predictive two zones model. To evaluate the quality of the injection phase in terms of mixture preparation and then to obtain realistic results from the one-dimensional analysis, 3D in-cylinder analyses have been performed to calibrate the GT-Power combustion model, as previously stated.

The calibration of the combustion was obtained by means of an iterative 1D-3D procedure on eight relevant working points, all in Wide Open Throttle (WOT) conditions, periodically verified in accordance with the modifications introduced to the engine. Boundary conditions for the 3D calculation were coherently generated from the one-dimensional model; after

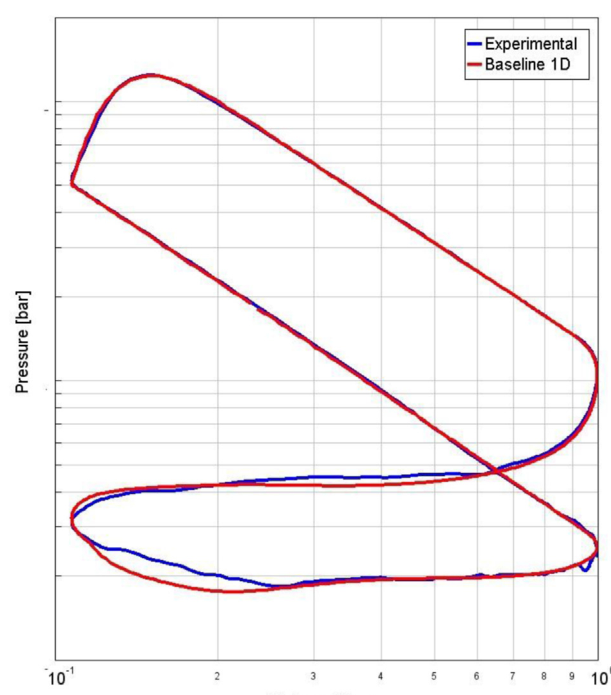


**Fig. 3 – Comparison between CFD-1D GT-Power results and experimental in-cylinder pressure measurements of the baseline engine. Cylinder 1.**

that, the CFD 3D combustion results were post-processed directly in GT-Power using the Three Pressure Analysis (TPA) method to correctly evaluate the actual law of burned fraction to be used in the 1D simulation. The TPA was preferred over the Stand-Alone Burn Rate Calculation by virtue of the possibility to calculate the residual fraction as well as the trapping ratio of the engine instead of estimating these values. In fact, using the intake and exhaust pressure curves (at the boundaries) and the 3D CFD in-cylinder pressure curve (see Chapter 4.2), the entire engine cycle is simulated. The Burn Rate is consequently obtained with an iterative calculation.

Finally, the burn rate is imposed in the one-dimensional code using a Wiebe function that best fits the burn rate identified with the TPA analysis. Knock limits conditions and Maximum Brake Torque (MBT) ignition timing were identified, for each working point investigated, by means of 1D-3D combustion loops. Moreover, these CFD-3D analyses showed that, at least in this specific hydrogen engine, some parameters, such as the tumble level or the local distribution of lambda, appear to have a marginal effect on the combustion process itself (i.e. Mass Fraction Burned curve), when the combustion event is properly phased, that is to say adjusting the spark timing on a case by case basis; for these parameters hence simplifying assumptions are allowed in first approximation. On the contrary, other parameters, such as the in-cylinder (mean) trapped value of lambda or the compression ratio exhibit a non-negligible effect on the combustion event and, consequently, can not be neglected. This whole procedure made the combustion behaviour mappable, giving reference points for the 1D codes. The combustion characteristics were ultimately interpolated among these verified points. It is worth remembering that overall capabilities of the models used in predicting the characteristics of hydrogen combustion are fundamental to obtain robust results. Based on this, analysis about the level of correlation between numerical and experimental results will be one of the most crucial future development of this activity.

Using the Knock Index (KI) dictated by the postprocessing of these pressure curves in the 1D model, a Knock Prediction model based on the Douad&Eyzat [47] correlation was implemented in the 1D model in conjunction with a Knock Control Strategy based on a Proportional–Integral–Derivative Controller (PID) able to postpone the Center of Combustion (CoC) (which is the anchor angle for the Wiebe law) in case of knock detection outside of the verified operating points. The entire methodology is schematically represented in Fig. 4.

Accurate nitrogen oxides prediction was performed only in 3D models since these detailed chemistry models [7] showed the inaccuracy of the 0D simplified Zeldovich *NOx* model (Ref [25], Section 11.2).

### *CFD-3D*

Combustion processes and complex local phenomena during the hydrogen injection phase were deeply investigated using 3D in-cylinder combustion simulations by making use of the commercial software CONVERGE CFD (v3.0.22), developed by Convergent Science Inc. The code solves the unsteady Reynolds-Averaged Navier Stokes (RANS) equations, closed by the RNG k-$\varepsilon$ turbulence model.

The strategy of the numerical simulations can be summarized as follows:

- A mesh grid is generated for the entire domain, comprising both the combustion chamber and the intake/exhaust ducts. The base size of the mesh is of 4 mm, while during the simulation some refinements are applied combining some fixed embedding (e.g. close to the injector location

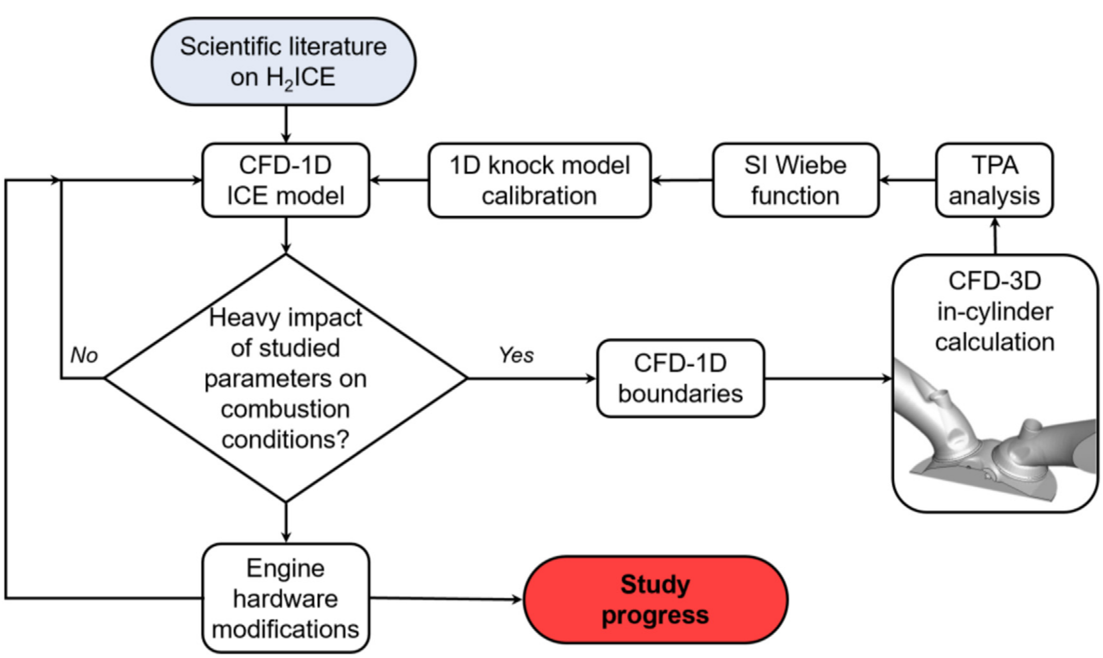


**Fig. 4 – Methodology used for the numerical investigation.**

and in proximity of the walls) and the Adaptive Mesh Refinement (AMR), based on the local gradients of velocity, temperature and hydrogen scalar. This makes the total number of cells variable during the simulation, in a range between 300′000 and 1′300′000 cells.

- The combustion model used in the simulation is the SAGE Detailed Chemistry solver offered by the CONVERGE software. The model solves detailed chemistry calculations to analyze the development of the combustion process in terms of species production and heat release. The mechanism chosen for the simulation counts 44 species and 250 reactions [7], since it is capable of capturing both performances and emissions aspects, with a contained computational cost.
- The wall heat transfer model used is the GruMo-UniMORE.
- Initial conditions, boundary conditions and surfaces temperatures are derived from the 1D model. The simulation starts before Exhaust Valve Opening (EVO).

Special attention was given to the mesh setup, since the hydrogen injection phenomenon reaches critical conditions at the injector outlet. Very high velocities can be measured in that area, with supersonic conditions experienced in the injector channels: this implies that a very fine mesh has to be used in order to be able to capture the details of the process. The simulation results were compared to the experimental results acquired using a SANDIA DI-*H2*ICE [34,48], modified to provide optical access to the combustion chamber. The experiment uses particle image velocimetry and planar laser-induced fluorescence to measure the velocity fields and the fuel mole-fraction, respectively. Measurements are performed in the central vertical symmetry plane of the cylinder.

Fig. 5 presents the progression of the fuel mixing during the compression phase. Comparing the evolution of the fuel mixture in terms of mole fraction between CONVERGE numerical model and the experimental results, it can be stated

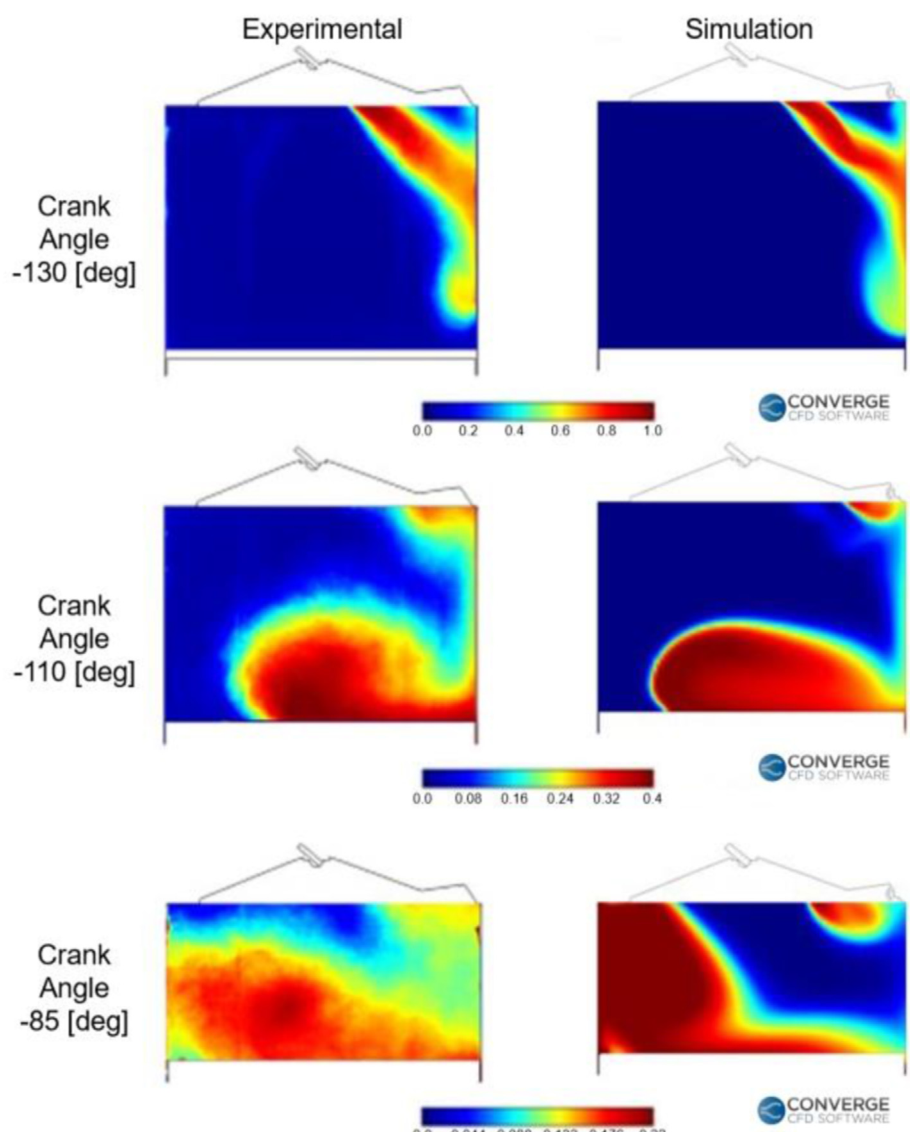


**Fig. 5 — Correlation between the CFD-3D calculation and the experimental reference case.**

that the mesh setup is fine enough to capture the phenomenon, both in terms of jet penetration and fuel impingement onto the liner wall, especially in the first phases of the injection.

The same numerical setup was extended to the presented case study and thus used to evaluate the mixing quality during the injection phase, to predict Heat Release Rate (HRR), Knock Limits, ignition limits and emissions production.

As far as the combustion process is concerned, no validation was performed for lack of relevant experimental data in the present study. However, it must be considered that the hydrogen combustion process involves the production of very few sub-products with respect to a standard gasoline combustion (mainly because of the lack of all the hydrocarbons mid-products), and this is testified by the reduced number of chemical reactions that can be found in the mechanisms for hydrogen. Moreover, another complexity reduction consists in the simplicity of the fuel, that is uniquely defined by the hydrogen molecule, while with gasoline a surrogate has to be found that is able to match its numerous properties (i.e. Lower Heating Value (LHV), Research Octane Number (RON), Motor Octane Number (MON), LFS, density, distillation curve). These considerations allowed the authors to hypothesize that the simulation of hydrogen combustion process can be considered as representative of the reality using a detailed chemistry approach, with a low degree of uncertainty. These simulations were then used to calibrate the combustion model of the 1D numerical code, as previously discussed.

## Numerical results and discussion

### *Hydrogen injection phase*

This first part of the study shows the effect of the injection process on the engine performance when fixed intake and in-cylinder mixture conditions are assumed, i.e. with the same levels of Manifold Absolute Pressure (MAP), Intake Air Temperature (IAT) and trapped lambda. It is essential to remember that results of this analysis are consistent with these boundary conditions, which means if the intake is limiting the performance of the engine. If, on the contrary, the target is a fixed value of torque (namely BMEP) the effect of the injection timing on the engine behaviour can produce different outcomes. Therefore, these findings appear crucial for the achievement of maximum performance in engine operating points where, due to insufficient volumetric efficiency, the power output, otherwise, would be deemed inappropriate.

Fig. 6a shows the effect of different Start Of Injection in a log(P)-log(V) diagram; the selected injector is rated for a static mass flow rate of 20 g/s. At the same time, Fig. 6b presents the in-cylinder pressure trace and the injection rate profile with three different values of injection timing. A detailed view of the pressure increment during the injection phase is also showed.

From an analysis of Fig. 6, it is apparent that a considerable contribution to performances is due to a lower compression work during the first part of the compression stroke.

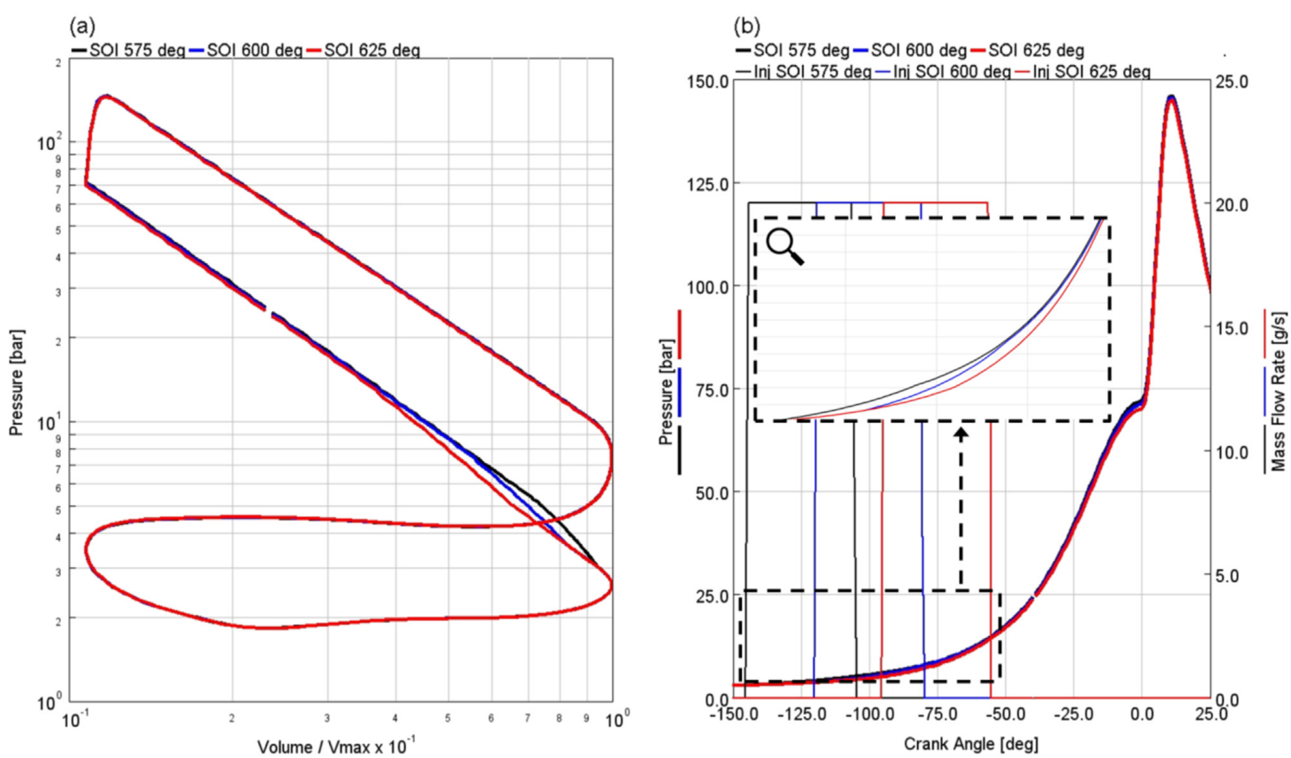


**Fig. 6 – Effect of the Start Of Injection on the engine operation. Log(P)-log (V/*Vmax*) (a), Cylinder Pressure (b) (Cylinder 1).**

Figs. 7 and 8 show the effect of a SOI sweep in a full load working point at a high engine speed for two distinct types of injectors, characterized by different mass flow rates, respectively 10 g/s and 20 g/s.

In particular, Fig. 7b directly presents the most interesting final result which is the BMEP; to correctly contextualize these data however, also the End Of Injection (EOI) is reported (Fig. 7a).

Fig. 8, on the other hand, closely reveals why the BMEP shows this trend, analyzing specific key parameters, in particular the Gross IMEP (a), the Brake Efficiency (b), the Normalized Heat Transfer (c), the Intersection Pumping Integral (d).

Targeting the same intake absolute pressure, the consequence is that the wastegate is adjusted differently in each simulated case resulting in different exhaust backpressure levels; scavenge motions during the overlap phase are not really affected by the wastegate (WG) position because the cam profile and the "reference" cam timing result in virtually no overlap. Full load conditions are achieved with a lambda trapped value of 2.0. Scientific publications in fact suggest to operate hydrogen fuelled engines with lambda value higher than 2.0 to guarantee low *NOx* values. Lower lambda values are critical because of *NOx* limits and pre-ignition occurrences. For this reason, in this phase, dilution of lambda 2.0 was defined as the lowest lambda value operable, i.e. the mixture value to use in WOT curve condition. Considering the fact that these preliminary calculations were obtained imposing a fixed value of combustion duration (10–90), the results should be interpreted choosing an end of injection

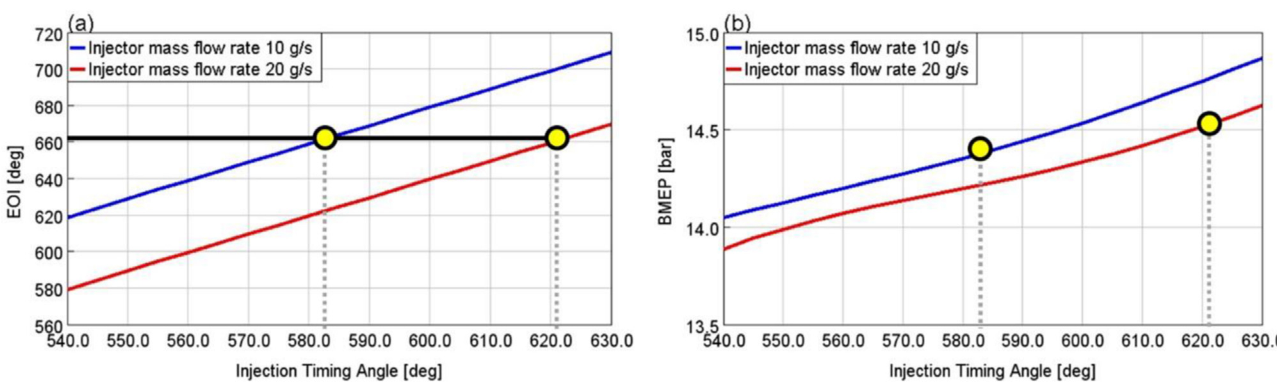


**Fig. 7 – Effect of a Start Of Injection sweep on the engine operation. EOI (a), BMEP (b).**

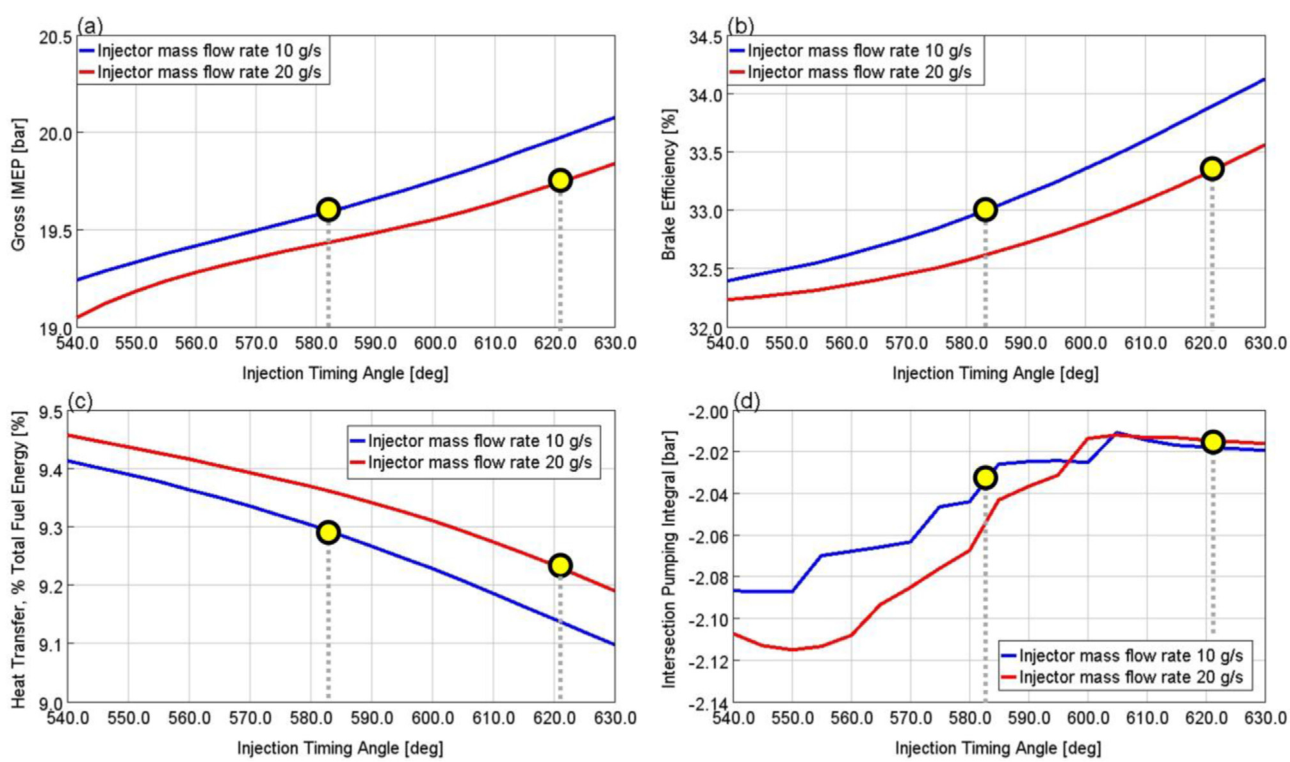


**Fig. 8 – Effect of a Start Of Injection sweep on the engine operation. Gross IMEP (a), Brake Efficiency (b), Normalized Heat Transfer (c), Intersection Pumping Integral (d).**

(EOI) limit for each injector type, depending mainly on diffusion and homogenization times. The selected value for the EOI, evinced from 3D analysis, is shown in Fig. 7 (black thick line) and the corresponding values of injection timing angle (i.e. SOI) are consequently defined for each type of simulated injector. Therefore, although the BMEP produced by the engine for a given value of SOI is higher for the case of low injection flow rate, the true comparison between the performance of the two injectors must be performed at same limits of EOI. Under this assumption, the resulting BMEP is higher for the case of high injection flow rate, since the injection can be delayed, thanks to its shorter duration. These EOI limits are then used to compare the effects of the two different injectors in Fig. 8.

Fig. 8 reports that for each injector type, delayed SOI instants produce good effects on both performance and efficiency, thanks to a drastic reduction of the work needed during the compression stroke. The injected hydrogen in fact tends to make the compression phase more burdensome; this aspect is also associated with increased values of maximum pressure at the TDC also in motored operation. From the discussion proposed describing Fig. 6, it can be clearly explained the reason why, inspecting Fig. 8a, the Gross IMEP continuously increases when delaying the SOI, despite being at fixed intake conditions and, more in detail, an almost constant quantity of trapped air in the cylinder at the IVC. To better highlight the aforementioned behaviour in terms of pumping efficiency, Fig. 8d shows the slight reduction of the Intersection Pumping Integral (i.e.the integral average during the negative cycle) for the 20 g/s case. A modest effect is also produced by a decrement in heat losses.

To support the rationale of this finding, it should be reminded that the 1D code used for this analysis is fitted with the Woshni GT heat transfer model, validated on the baseline engine bench measurements. With this type of heat transfer model, the mean fluid speed of the flow within the cylinder, needed for the calculation of the heat transfer coefficient, is calculated as a function of the instantaneous pressure and temperatures values during the compression stroke. All these parameters are influenced by the injection event itself as well as the instantaneous composition of the fluid, producing a dependency which is, according to the authors, the most consistent possible at this level of numerical investigation. In conclusions, the effect of the SOI timing, with the aforementioned fixed intake conditions and mixture composition constraints, could result in considerable gains in terms of BMEP. After these first outcomes, authors selected some specific operating points and submitted them to accurate 3D calculations (cold flow and combustion analyses). Results showed that, with the same injector nozzle geometry among all cases, the mixture preparation is affected by the SOI event but, choosing the appropriate advance timing for each case, the combustion process itself is only marginally affected. This outcome hence supports that, at first instance, the effect of the injection timing can be investigated via 1D tools. Accordingly, these results drove the selection of the right injector nozzle geometry to use for the rest of the investigation. Within this work, the definition of this key component requirements implies the selection of a specific injector geometry for in-cylinder simulations and the beginning of the 1D-3D combustion loops needed to calibrate the one-dimensional combustion model against 3D results.

### *Turbine discharge pressure*

As already stated, average EU6 turbocharged GDI engine levels of turbine discharge pressure can be excessive and not representative for a lean burn hydrogen application. Thus, with the present analysis, the effect on the engine behaviour of the four different exhaust lines presented in Chapter 3.2 is discussed. Numerical results are reported here for an operating point at high engine speed and high load, close to the maximum power; in these conditions in fact the effect of the backpressure is more evident as a consequence of the high volume flow rates elaborated. The wastegate actuator was adjusted targeting the same level of Manifold Absolute Pressure in this case as well. Once again, it is worth remembering that results of this analysis are consistent with the aforestated fixed intake and dilution conditions. Fig. 9 shows the results when modelling the exhaust line under different assumptions. In particular, presented parameters are BMEP (9a), Brake efficiency (9 b), Intersection Pumping Integral (9c). Fig. 9d displays the corresponding working point on the turbine map.

From numerical simulations, it is clear that with fixed intake conditions, a reduced value of turbine discharge pressure contributes to an improvement in brake efficiency. It is important to highlight that the gain in pumping efficiency is so relevant to produce this result besides the fact that the working point within the turbine operating map moves towards lower value of total-to-static efficiency, as it is visible in Fig. 9d. As concerns compressor, in the present case, it appears totally appropriate for this application and, targeting the same MAP condition, its operating point is marginally affected by the exhaust line fitted. It is worth pointing out that, in all cases, the Turbine Entry Temperature (TET) is around 700 °C. Similarly to conventional ICEs, hydrogen engines exhaust gas temperature tends to show a strong correlation to the air/fuel ratio. As a consequence, the low value of temperature at the turbine inlet is a direct consequence of the oxygen excess (mixture at lambda 2.0). It is worth reminding that the simulated point showed in Fig. 9 is in the higher range of the engine speed, while lower engine speed operating points, at the same level of lambda, exhibit further lower TET values. In general, such values of TET are the main cause of the difficulties in boosting at low engine speeds. Considering these results, it appears reasonable that with different engine design constraints (full load lambda or hybrid powertrain layout, as stated in Chapter 2) a specific turbocharger design in order to achieve a more suitable matching on the operating map could result in further improved performances. It should be also remarked that these exhaust temperatures are compatible with Variable Geometry Turbocharger (VGT) technology that could bring to further improvements thanks to a better utilization of exhaust gas exergy. Within the present study however, for the reasons stated above, authors decided to maintain a fixed geometry turbocharger controlled by means of a wastegate actuator.

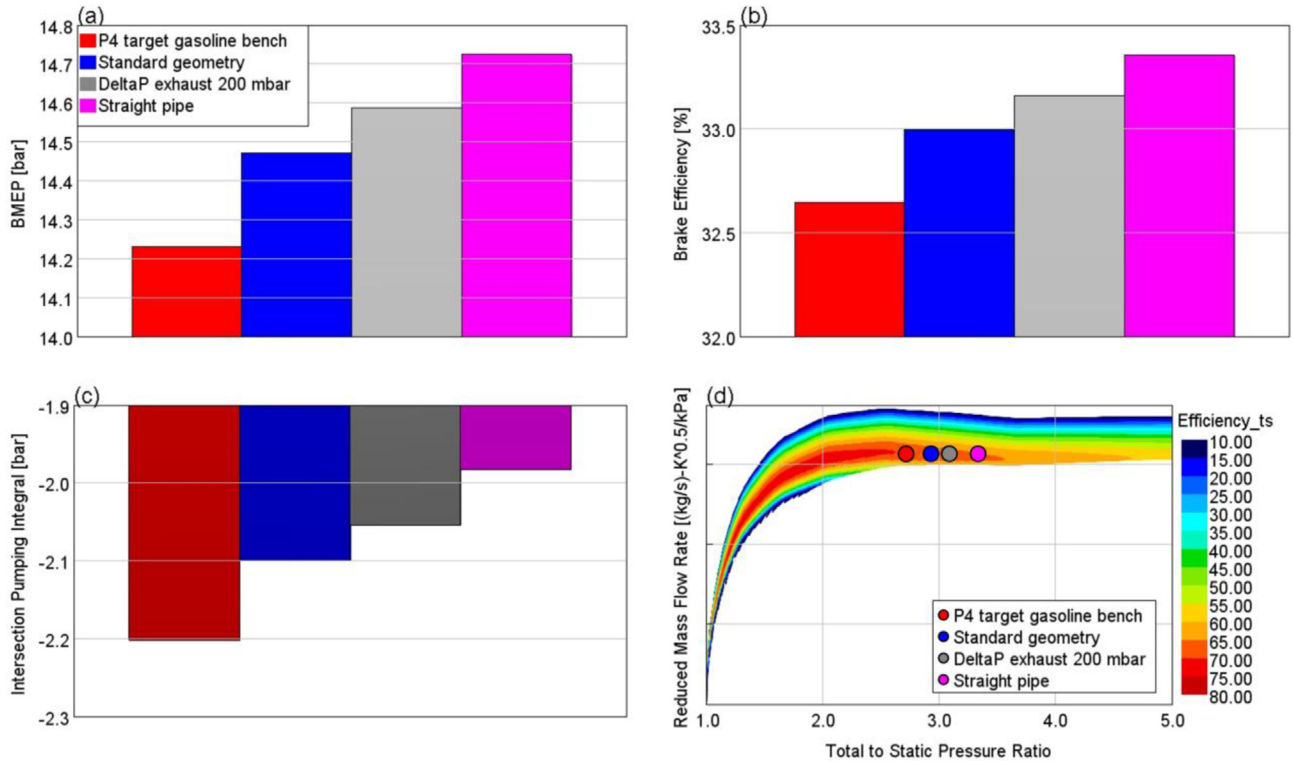


**Fig. 9 – Effect of a Start Of Injection sweep on the engine operation. BMEP (a), Brake Efficiency (b), Intersection Pumping Integral (c), Turbine Map (d).**

### *Compression ratio effect*

Detailed calculations computed by means of 3D combustion codes showed the complete absence of knock with the standard compression ratio (9.3:1) also operating significantly beyond Maximum Brake Torque ignition timing targeting the desired torque curve. This fact appears to the authors as a consequence of two interesting aspects: the first one is that the boost pressure is moderate in the LET zone, due to the low enthalpy at the turbine inlet, which causes low compressor pressure ratios and consequently low trapped air masses. The second aspect is that the LFS of hydrogen mixtures, even at lambda 2.0, is far higher than that of gasoline-air mixtures, thus resulting in a weaker dependence of knock tendency with respect to the charge turbulence level and so to the engine speed.

Fig. 10 shows the main differences along all the full load curve increasing the nominal Compression Ratio from 9.3:1 to 12.0:1. Specifically, the selected quantities are: BMEP (10a), Brake Efficiency (10 b), Indicated Efficiency (10c), Average Maximum Cylinder Pressure (10d).

It is worth reminding that the wastegate actuator was adjusted to target the desired torque curve; this means that curves are at the same level of torque whenever the intake pressure in both cases is sufficient to guarantee the performance and at different levels of performance, with the wastegate completely closed, at low engine speeds. All the presented results were generated considering the effect of the new CR on the combustion process; the Wiebe law used for the one dimensional code was properly adjusted in each case based on 3D calculations and TPA analysis results.

Inspecting Fig. 10, the following observations were made: numerical calculations confirm the expected increase of indicated efficiency and, more importantly, brake efficiency; when increasing the compression ratio, although heat transfer rates are higher, the indicated efficiency rises. In terms of brake efficiency, the effect is mitigated by an increased FMEP (i.e. reduced organic efficiency). Using the Chen-Flynn friction correlation within the one-dimensional code, experimentally validated over the baseline engine bench data, the effect of in-cylinder pressure is accounted in the FMEP estimation. Maximum cylinder pressure and temperatures are associated with higher *NOx* emissions that, however, are still below critical values as a consequence of oxygen excess. The main drawback of this modification is a reduction of full load performance in the LET zone. In fact, the aforementioned low level of enthalpy at the turbine entry indeed further deteriorates, due to a lengthened expansion phase. In confirmation of this, numerical investigations hypothesizing a delay of the ignition timing, showed a beneficial effect on boost buildup and, as a direct consequence, in brake torque. Moreover, delayed spark timing are associated with lower pressure peaks within the combustion chamber, with desirable effects on frictions and *NOx* production. This fact is especially true for hydrogen engines where, for the abovementioned physical reasons, the combustion process is exceptionally fast, with short heat release rate durations and therefore high cylinder pressure peaks. In conclusion, in spite

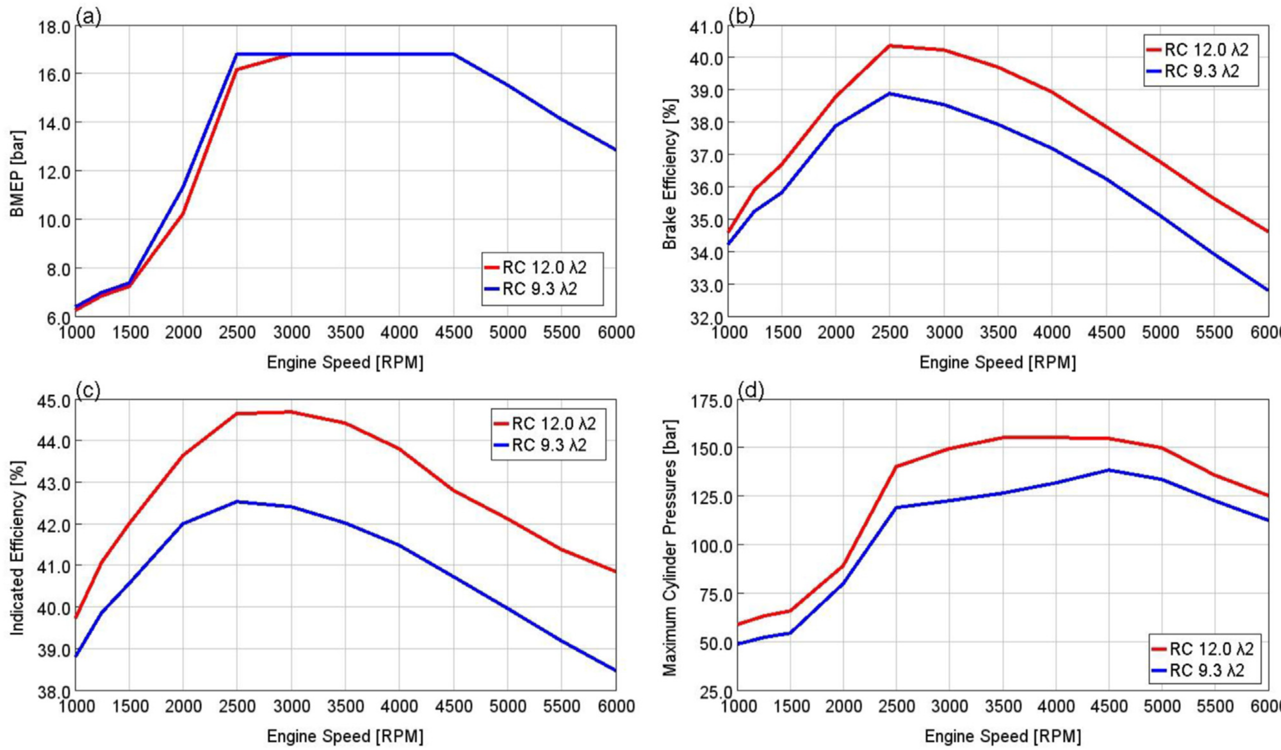


**Fig. 10 – Effect of different nominal compression ratio values on full load performances. BMEP (a), Brake Efficiency (b), Indicated Efficiency (c), Average Maximum Cylinder Pressure (d).**

of a small BMEP reduction at low engine speeds, the overall efficiency of the engine is greatly increased. Even now, anyway, it is important to clarify that the turbomatching for this *H2* application of the ICE was defined considering the target power output, a mixture dilution equivalent to lambda 2.0 at the top end in full load and a safety margin from the choke line; this means that a different turbocharger, still using the same technology level, can not be selected to improve the low end torque without affecting the maximum power output.

### NOx *emissions and lambda sensitivity*

As already mentioned in Section 3.4, the 3D results were post-processed with the aim of using relevant findings to indirectly control nitrogen oxides production within the onedimensional model. Fig. 11 shows the predicted *NOx* raw emissions from CFD combustion calculations at different engine points. All evaluated cases were at an engine speed of 2000 rpm with different levels of valve overlap and different values of trapped lambda at the Intake Valve Closure (IVC).

For each operating point a spark sweep until reaching the knock limit was numerically simulated. The main outcome is a clear and strong correlation between the maximum cylinder pressure and the *NOx* raw emission. Although this consideration could appear obvious, it really is not the case. In fact, the analysis showed that the effect on *NOx* production of internal exhaust gas recirculation, lambda trapped, effective CR (IVC affected) and spark timing are completely described from the maximum cylinder pressure value reached, roughly regardless of how much each phenomenon is responsible for the final *NOx* raw emission. *NOx* emissions are hence highly sensitive to changes in the relative air/fuel ratio but the different control of the intake stroke or of the combustion phasing tends to evidently weaken the dependency from just this parameter. These considerations thus drove the definition of maximum cylinder pressure thresholds to constrain, by means of a PID controller, the one-dimensional code. By doing so, it was possible to optimize the scavenge and the effective trapped lambda in such low speed zone in order to identify feasible and favourable operating points. The presented aspect is of absolute practical relevance because it allows a simplified and less time-consuming utilization of the

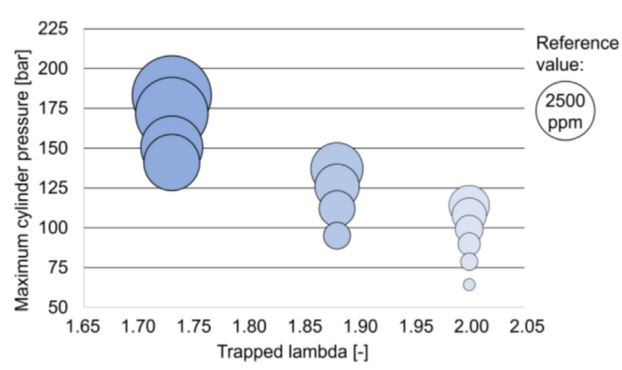


**Fig. 11 – Raw *NOx* emissions at 2000 rpm. Spark Timing sweep of three different operating points at distinct values of trapped lambda (respectively: 1.73, 1.88, 2.0) and VVT regulation.**

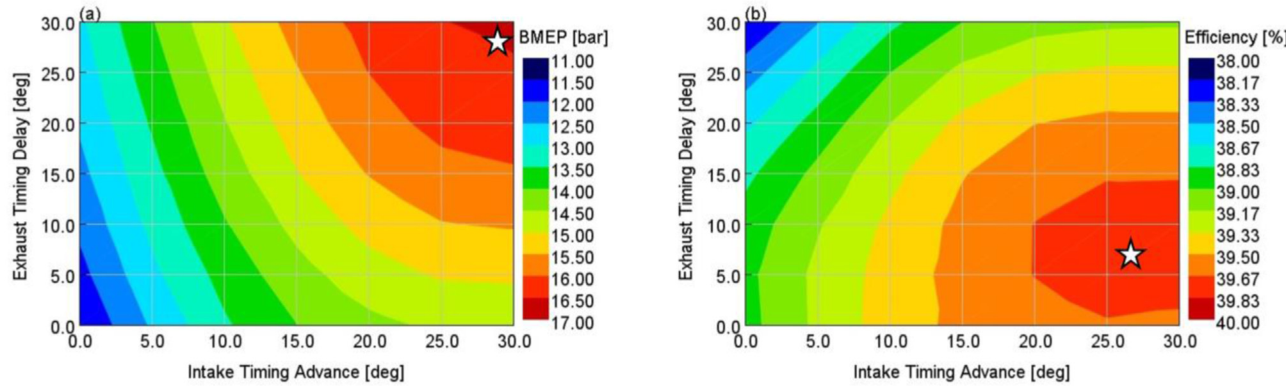


**Fig. 12 – Contour map of BMEP (a) and Brake Efficiency (b) as a function of the Intake Timing Advance and Exhaust Timing Delay. Engine speed: 2000 rpm. Trapped lambda: 1.8.**

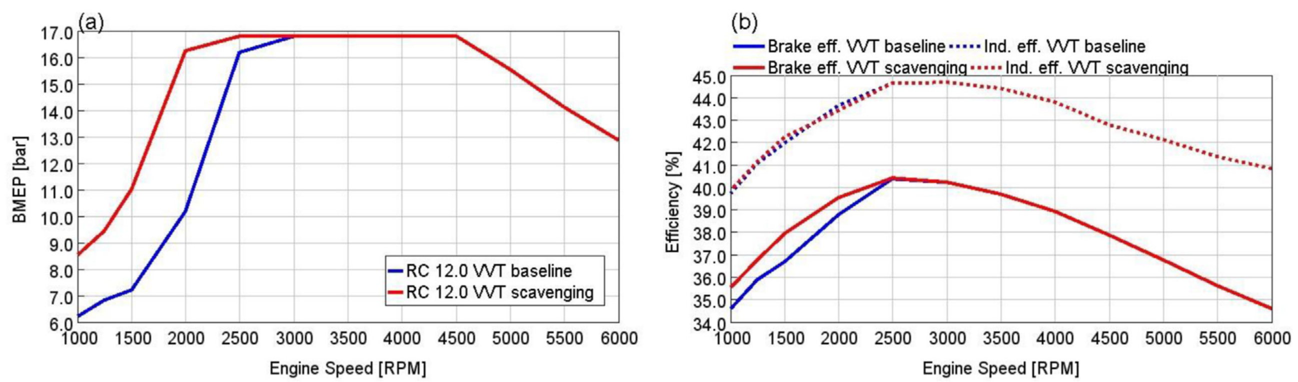


**Fig. 13 – Effect of the use of proposed LET strategies on full load performances. BMEP (a), Brake and Indicated Efficiency (b).**

1D code to evaluate different possible working conditions, highly reducing the demand for detailed 3D verifications (i.e. 1D-3D loops).

### *LET performance and scavenging*

As previously stressed, the performance at low engine speeds is poor if compared with modern gasoline engines. Consequently, a Design Of Experimenents (DOE) methodology was performed in order to evaluate individual and combined effects of the strategies presented in Chapter 3.5. As outlined there, both intake and exhaust cam timings were concomitantly used to induce scavenging on the engine, while angular adjustment limits were defined according to the maximum valve lift permitted at the TDCe. The one dimensional code was constrained by means of two PID controllers. The first one performs in the case of knock detection by postponing the combustion anchor angle for the Wiebe law. The second one limits the maximum cylinder pressure, as an indirect way to control the *NOx* raw emission, by operating on the boost level through the wastegate actuator.

Fig. 12 shows the trends in BMEP (12a) and Brake Efficiency (12 b) as a function of the Intake Timing Advance (ITA) and Exhaust Timing Delay (ETD). In each figure, a star highlights the optimal value.

Fig. 13 displays reachable BMEP (13a) and efficiency (brake and indicated) (13 b) values along the whole full load curve thanks to the use of these strategies in the LET zone.

From a perusal of Fig. 12 it can be noted that, for the pure performance, this engine demands maximum ETD and ITA; going in this direction, in fact, the air short circuit increases and the Pressure Ratio of the compressor rises considerably. On the other hand, extreme values of exhaust delay are associated with an expansion stroke that persists too far,

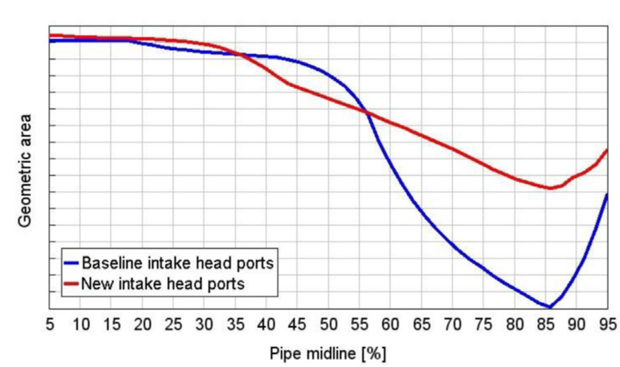


**Fig. 14 – Total geometric area of the intake port duct progressing during the pipe midline.**

hampering the quality of the natural exhaust phase. Brake efficiency (12 b) hence shows a maximum for low ETD values. As a result, the performance (BMEP) can be strongly enhanced when introducing an adequate level of scavenge and reducing the mixture dilution from lambda 2.0 to 1.88, as clearly visible in Fig. 13. The aforesaid (Chapter 5.4) indirect *NOx* control strategy has proved reliable and robust since the subsequent 3D analysis confirmed a level of *NOx* production utterly consistent with expectations.

### *Intake head ports design*

As specified above, contrary to GDI engines, high tumble ports appear unnecessary in the case of hydrogen engines developed in view of operating with lean mixtures and high efficiency. On these bases, new intake ducts were designed and analyzed.

Fig. 14 shows a comparison of the evolution of the geometric port area as a function of the normalized midline length for both ports geometries. For reasons of confidentiality, dimensional data have been removed; both graphs anyway share the same scale, hence Fig. 14 relative variation can be compared.

The new geometry was designed exploiting the internal know-how on high flow naturally-aspirated engines. With this design, the tumble level is roughly one-third of that of the baseline one and the permeability is appreciably higher. Nevertheless, the new shape is completely compatible with the baseline head castings. Valves, valve seats and valve guides positions are exactly the same between the two geometry and the entire valvetrain layout is hence unaffected. A future experimental validation of the proposed layout is consequently easily feasible.

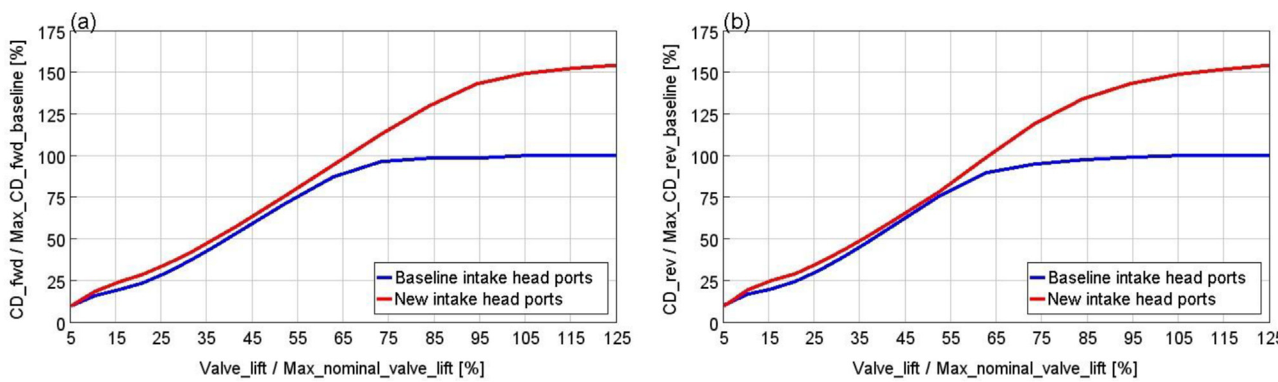


**Fig. 15 – Forward (a) and Reverse (b) Discharge Coefficients for the old and new exhaust ports (fixed reference area: bore). Data normalized over the maximum value provided with the baseline geometry.**

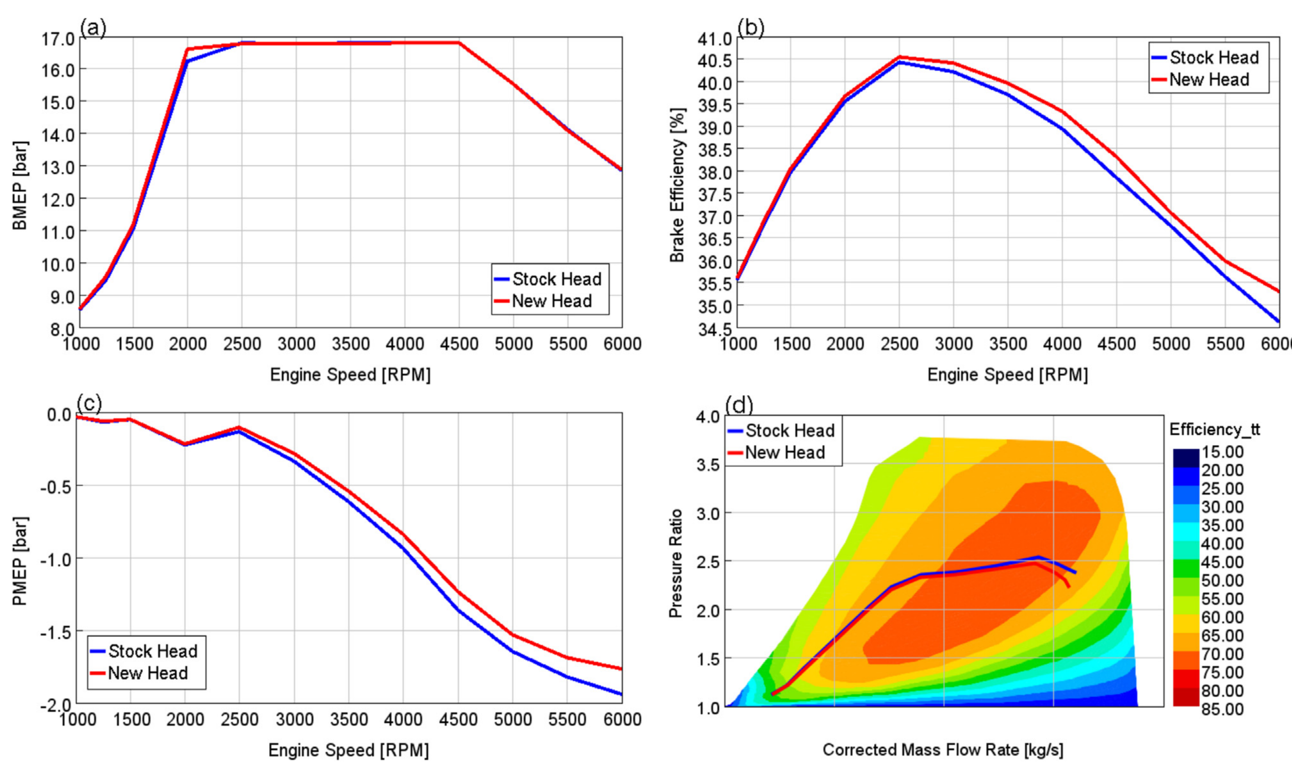


**Fig. 16 – Effect of the use of proposed LET strategies on full load performances. BMEP (a), Brake and Indicated Efficiency (b).**

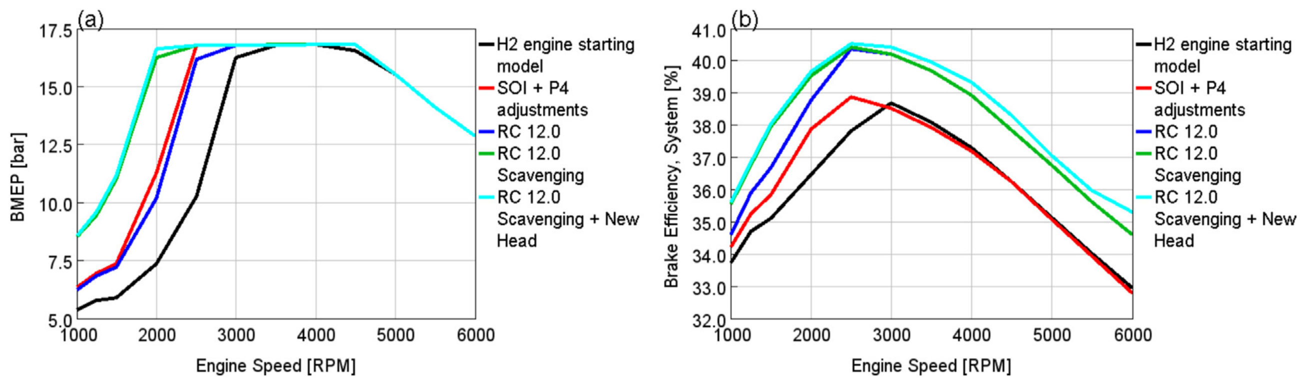


**Fig. 17 – Main evolution of the engine performance during the presented study. BMEP (a), Brake Efficiency (b).**

Fig. 15 presents discharge coefficients in the direction of the flow and in the reverse one (referenced to the bore) for the new ducts geometry compared with the old one, both as a function of the valve lift normalized on the maximum lift provided from the baseline cam profile.

For both geometries, these results were obtained with a numerical steady state flushing (CFD code: Star-CCM+) using the same numerical setup.

The improvement guaranteed by the new solution is increasingly noticeable towards higher valve lift values, since the throat area moves toward the port.

Fig. 16, reveals how the new intake ports design affects the performance. In particular, reported quantities are BMEP (16a), Brake Efficiency (16 b), PMEP (16c), Compressor operating points (16d).

From a perusal of Fig. 16, it is clear that at low engine speeds an improvement is accomplished with the new intake ports. However, the effect is modest because the airflow demand of the engine in these operating zones is moderate. On the contrary, at higher engine speeds the effect is substantial and, limiting the torque output at the required value, the positive effect is noticeable in terms of efficiency.

## Summary of results

Fig. 17 shows in brief the main evolutions of the engine performances progressing with the study. Specifically, the selected quantities are: BMEP (17a) and Brake Efficiency (17 b).

From a perusal of Fig. 17, it is apparent that the objective of optimizing the BMEP in the low speeds zone without affecting maximum brake power output, is successfully achieved. Every proposed modification to the engine directly translates into an increase in brake efficiency. Trends proposed in Fig. 17 hence confirm the eligibility of the expected hardware modifications to adapt the engine operation according to the hydrogen fuel properties and requirements.

## Conclusions

In the present study, an extensive numerical investigation was performed in view of a re-design of an existing gasoline engine into a hydrogen fuelled one. A well-known, robustly correlated CFD-1D engine model was adopted in order to quantitatively evaluate major consequences in developing innovative turbocharged internal combustion engines fuelled by means of lean burn hydrogen-air mixtures.

Specifically, the test case of the present study is a high performance turbocharged GDI engine. CFD-1D simulations were carried out using the commercial software GT-Power (v2016), while the model construction and validation were supported by steady state CFD-3D analysis performed using Star-CCM+ (v15.06) software. The combustion process of hydrogen mixtures was simulated via CFD-3D employing commercial software CONVERGE CFD (v3.0.22).

The numerical setup was purposefully calibrated, in terms of both mixture preparation and combustion occurrence, over a reference case dataset: an experimental investigation of an optical access engine reported in literature. To assess the overall capabilities of the model in predicting the characteristics of hydrogen combustion, numerical results will be compared with experimental results in future activities.

From the present study, the following evidences are proposed:

- High mass flow rate injectors and late injection timings are required to assure a good volumetric efficiency and to reduce the compression work.
- A specific exhaust line in conjunction with a rescaling of the turbocharger is necessary to guarantee an appropriate torque curve.
- For lean mixture *H2ICEs* higher compression ratio, with respect to gasoline engines, can be adopted. This modification lead to a widespread increment of the brake efficiency.
- *NOx* raw emissions tend to be moderate at dilution of lambda 2.0. There is a strong correlation between the maximum cylinder pressure and the *NOx* raw emissions, even reducing the lambda.
- In this type of engines, the Low End Torque zone performance tends to be modest; the main cause of this fact is ascribable to the low turbine inlet enthalpy. Scavenging techniques can help addressing these drawbacks.
- Thanks to a lesser need for high turbulence to guarantee a fast burning rate, the design of intake head ports can be focused on a high permeability, ensuring better performance in terms of brake efficiency.

## CRediT author statement

**Alessio Anticaglia:** Conceptualization, Methodology, Software, Validation, Investigation, Data curation, Writing- Original Draft.

**Francesco Balduzzi:** Visualization, Methodology, Supervision, Writing- Review & Editing.

**Giovanni Ferrara:** Resources, Methodology, Supervision, Project administration.

**Michele De Luca:** Conceptualization, Methodology, Software, Technical Supervision, Project administration.

**Davide Carpentiero, Alessando Fabbi:** CFD-3D In-cylinder and combustion Investigation, Software and Numerical Setup.

**Lorenzo Fazzini:** Vehicle driving cycle Investigation.

## Declaration of Competing Interest

The authors declare that they have no known competing financial interests or personal relationships that could have appeared to influence the work reported in this paper.

## Acknowledgements

The Authors wish to thank their colleagues at HPE-COXA for their help and support for this work. In particular: Mr. Stefano Pellegrini and Mr. Simone Mongiardo, Engine Performance CFD-1D engineers.

REFERENCES

[1] Candelaresi D, Valente A, Iribarren D, Dufour J, Spazzafumo G. Comparative life cycle assessment of hydrogen-fuelled passenger cars. Int J Hydrogen Energy 2021;46(72):35961–73. https://doi.org/10.1016/j.ijhydene.2021.01.034. 2021.

[2] Kumar Vasu, Gupta Dhruv, Kumar Naveen. Hydrogen use in internal combustion engine: a review. International Journal of Advanced Culture Technology 2015;3(2):87–99.

[3] Timmers Victor RJH, Peter AJ Achten. Non-exhaust PM emissions from electric vehicles. Atmos Environ 2016;134:10–7. https://doi.org/10.1016/j.atmosenv.2016.03.017.

[4] Salazar Victor M, Kaiser Sebastian A. Characterization of mixture preparation in a direct-injection internal combustion engine fueled with hydrogen using PIV and PLIF. In: 15th int. Symp. On application sof laser techniques to fluid mechanics; 2010. Lisbon, Portugal.

[5] Addepalli Srinivasa Krishna, et al. Multi-dimensional modeling of mixture preparation in a direct injection engine fueled with gaseous hydrogen. Int J Hydrogen Energy 2022;47(67):29085–101. https://doi.org/10.1016/j.ijhydene.2022.06.182.

[6] Yamane Kimitaka, et al. A development of a high pressure H2 gas injector with high response by using common-rail injection system for direct injection H2 fuelled engines. In: 16th world hydrogen energy conference; 2006.

[7] Zhang Yingjia, et al. Assessing the predictions of a NOx kinetic mechanism on recent hydrogen and syngas experimental data. Combust Flame 2017;182:122–41. https://doi.org/10.1016/j.combustflame.2017.03.019.

[8] Krebs Sören, Biet Clemens. Predictive model of a premixed, lean hydrogen combustion for internal combustion engines. Transport Eng 2021;5:100086. https://doi.org/10.1016/j.treng.2021.100086.

[9] Ng Hoi Dick, Ju Yiguang, Lee John HS. Assessment of detonation hazards in high-pressure hydrogen storage from chemical sensitivity analysis. Int J Hydrogen Energy 2007;32(1):93–9. https://doi.org/10.1016/j.ijhydene.2006.03.012.

[10] Kawahara Nobuyuki, Tomita Eiji, Roy Mithun Kanti. Visualization of autoignited kernel and propagation of pressure wave during knocking combustion in a hydrogen spark-ignition engine. SAE Technical Papers 2009. https://doi.org/10.4271/2009-01-1773.

[11] Dahoe AE. Laminar burning velocities of hydrogen–air mixtures from closed vessel gas explosions. J Loss Prev Process Ind 2005;18(3):152–66. https://doi.org/10.1016/j.jlp.2005.03.007.

[12] Verhelst Sebastian, Vancoillie J, Demuynck J. A correlation for the laminar burning velocity for use in hydrogen spark ignition engine simulation. Int J Hydrogen Energy 2011;36(1):957–74. https://doi.org/10.1016/j.ijhydene.2010.10.020.

[13] Salvi BL, Subramanian KA. A novel approach for experimental study and numerical modeling of combustion characteristics of a hydrogen fuelled spark ignition engine. Sustain Energy Technol Assessments 2022;51:101972. https://doi.org/10.1016/j.seta.2022.101972.

[14] Boretti A. Latest concepts for combustion and waste heat recovery systems being considered for hydrogen engines. Int J Hydrogen Energy 2013;38:3802–7. https://doi.org/10.1016/j.ijhydene.2013.01.112.

[15] Dong Chen, et al. Experimental study on the laminar flame speed of hydrogen/natural gas/air mixtures. Front Chem Eng China 2010;4:417–22.

[16] Unni Jayakrishnan Krishnan, Govindappa Premakumara, Das Lalit Mohan. Development of hydrogen fuelled transport engine and field tests on vehicles. Int J Hydrogen Energy 2017;42(1):643–51. https://doi.org/10.1016/j.ijhydene.2016.09.107.

[17] Miller Arthur L, et al. Role of lubrication oil in particulate emissions from a hydrogen-powered internal combustion engine. Environ Sci Technol 2007;41(19):6828–35. https://doi.org/10.1021/es070999r.

[18] Nogami Mai, et al. Development of a common-rail type high pressure hydrogen injector with a large injection rate and an ability of multiple stage injection. In: 18th world hydrogen energy conference; 2010.

[19] Dwivedi Sandeep Kumar, Vishwakarma Manish. Hydrogen embrittlement in different materials: a review. Int J Hydrogen Energy 2018;43(46):21603–16. https://doi.org/10.1016/j.ijhydene.2018.09.201.

[20] Ceper, Albayrak Bilge. Experimental investigation of the effect of spark plug gap on a hydrogen fueled SI engine. Int J Hydrogen Energy 2012;37(22):17310–20. https://doi.org/10.1016/j.ijhydene.2012.08.070.

[21] Baines Nicholas C. Fundamentals of turbocharging, 1. White River Junction, VT: Concepts NREC; 2005.

[22] Watson N, Janota M. Turbocharging the internal combustion engine. Macmillan International Higher Education; 1982.

[23] Augusto Pignone Giacomo, Vercelli Ugo Romolo. Motori ad alta potenza specifica. Nada; 2016.

[24] Ferrari G. Motori a combustione interna. Società Editrice Esculapio; 2019.

[25] Heywood John B. Internal combustion engine fundamentals. McGraw-Hill Education; 2018.

[26] Checcucci Matteo, et al. An integrated design approach for turbocharger turbines based on the performance optimization in transitory conditions. In: Turbo expo: power for land, sea, and air, 51173. American Society of Mechanical Engineers; 2018. https://doi.org/10.1115/GT2018-76719.
[27] Becciani Michele, et al. A pre-design model to estimate the effect of variable inlet guide vanes on the performance map of a centrifugal compressor for automotive applications. No. 2017-24-0020. SAE Technical Paper; 2017. https://doi.org/10.4271/2017-24-0020.
[28] Shadidi Behdad, Najafi Gholamhassan, Yusaf Talal. A review of hydrogen as a fuel in internal combustion engines. Energies 2021;14(19):6209. https://doi.org/10.3390/en14196209.
[29] Yip Ho Lung, et al. A review of hydrogen direct injection for internal combustion engines: towards carbon-free combustion. Appl Sci 2019;9(22):4842. https://doi.org/10.3390/app9224842.
[30] Wimmer Andreas, et al. H2-direct injection–a highly promising combustion concept. 2005. https://doi.org/10.4271/2005-01-0108. No. 2005-01-0108. SAE technical paper.
[31] Koch Daniel, et al. Simulation-supported development of a hydrogen engine for emission-free transport. MTZ worldwide 2017;78(11):36–41.
[32] Yang Zhenzhong, et al. Effects of injection mode on the mixture formation and combustion performance of the hydrogen internal combustion engine. Energy 2018;147:715–28. https://doi.org/10.1016/j.energy.2018.01.068.
[33] Optimization of the hydrogen internal combustion engine. In: Summary of an integrated Project in the 6th framework programme of the European commission; February 2007.
[34] Le Moine, Jerome, et al. A computational study of the mixture preparation in a direct–injection hydrogen engine. J Eng Gas Turbines Power 2015;137(11). https://doi.org/10.1115/1.4030397.
[35] Rosati MF, Aleiferis PG. Hydrogen SI and HCCI combustion in a direct-injection optical engine. SAE International Journal of Engines 2009;2(1):1710–36.
[36] Gao Jianbing, et al. Review of the backfire occurrences and control strategies for port hydrogen injection internal combustion engines. Fuel 2022;307:121553. https://doi.org/10.1016/j.fuel.2021.121553.
[37] Salvi BL, Subramanian KA. Experimental investigation on effects of compression ratio and exhaust gas recirculation on backfire, performance and emission characteristics in a hydrogen fuelled spark ignition engine. Int J Hydrogen Energy 2016;41(13):5842–55. https://doi.org/10.1016/j.ijhydene.2016.02.026.
[38] Plettenberg IM. Reliability solutions for hydrogen internal combustion engines. In: The 10th international conference of ICE reliability technology; 23 April 2021.
[39] Li Xiang-yu, et al. Experimental study on the cycle variation characteristics of direct injection hydrogen engine. Energy Convers Manag X 2022;15:100260. https://doi.org/10.1016/j.ecmx.2022.100260.
[40] Raser Bernhard, MartinWieser Fritz Grabner. CO2 reduction in commercial vehicles the avl hydrogen engine. In: AVL presentation; 2 March 2021.
[41] Heindl René, et al. New and innovative combustion systems for the $H_2$–ICE: compression ignition and combined processes. SAE International Journal of Engines 2009;2(1):1231–50.
[42] Sterlepper Stefan, et al. Concepts for hydrogen internal combustion engines and their implications on the exhaust gas aftertreatment system. Energies 2021;14(23):8166. https://doi.org/10.3390/en14238166.
[43] Oh Seungmook, et al. Analysis of the exhaust hydrogen characteristics of high-compression ratio, ultra-lean, hydrogen spark-ignition engine using advanced regression algorithms. Appl Therm Eng 2022;215:119036. https://doi.org/10.1016/j.applthermaleng.2022.119036.
[44] Mogi Yuki, et al. Effect of high compression ratio on improving thermal efficiency and NOx formation in jet plume controlled direct-injection near-zero emission hydrogen engines. Int J Hydrogen Energy 2022;47(73):31459–67. https://doi.org/10.1016/j.ijhydene.2022.07.047.
[45] Bao Ling-zhi, Sun Bai-gang, Luo Qing-he. Optimal control strategy of the turbocharged direct-injection hydrogen engine to achieve near-zero emissions with large power and high brake thermal efficiency. Fuel 2022;325:124913. https://doi.org/10.1016/j.fuel.2022.124913.
[46] McAllister Sara, Jyh-Yuan Chen, Carlos Fernandez-Pello A. Fundamentals of combustion processes, 302. New York: Springer; 2011.
[47] Douaud A, Eyzat P. Four-octane-number method for predicting the anti-knock behavior of fuels and engines. SAE Trans 1978;87:294–308. Section 1: 780006–780229 (1978).
[48] Salazar Victor M, Kaiser Sebastian A. Characterization of mixture preparation in a direct-injection internal combustion engine fueled with hydrogen using PIV and PLIF. In: 15th int. Symp. On application sof laser techniques to fluid mechanics; 2010. Lisbon, Portugal.